

## X-RAY ICS SOURCE BASED ON MODIFIED PUSH-PULL ERLS

I. Drebot\*, A. Bacci, A. Bosotti, F. Broggi, S. Cialdi, L. Faillace, D. Giannotti,  
D. Giove, P. Michelato, L. Monaco, R. Paparella, F. Prelz, M. Rossetti Conti, A. R. Rossi, L. Serafini,  
D. Sertore, M. Statera, V. Torri, INFN, Milano, Italy  
V. Petrillo, Università degli Studi di Milano & INFN, Milano, Italy  
G. Galzerano, E. Puppini, Politecnico di Milano, Milano, Italy  
A. Esposito, A. Gallo, C. Vaccarezza, INFN/LNF, Frascati Roma, Italy  
G. Mettievier, P. Russo, A. Sarno, Università di Napoli, Napoli, Italy  
P. Cardarelli, M. Gambaccini, G. Paternó, A. Taibi, Università di Ferrara & INFN, Ferrara, Italy

### Abstract

We present the conceptual designs of BriXS and BriXSinO (a minimal test-bench demonstrator of proof of principle) for a compact X-ray Source based on innovative push-pull ERLs. BriXS, the first stage of the Marix project, is a Compton X-ray source based on superconducting cavity technology with energy recirculation and on a laser system in Fabry-Pérot cavity at a repetition rate of 100 MHz, producing 20-180 keV radiation for medical applications. The energy recovery scheme based on a modified folded push-pull CW-SC twin Linac ensemble allows to sustain MW-class beam power with almost just one hundred kW active power dissipation/consumption.

### INTRODUCTION

BriXS (Bright and compact X-ray Source) [1] is a twin Compton X-ray source based on superconductive cavities technology for the electron beam with energy recirculation and on a laser system in Fabry-Pérot cavity at a repetition rate of 100 MHz, producing 20-180 keV radiation.

It has been conceived as the first acceleration stage of the X-ray FEL MariX [2,3]. MariX is an X-ray FEL based on the innovative design of a two-pass two-way superconducting linear electron accelerator, equipped with an arc compressor to be operated in CW mode at 1 MHz.

The double Compton X-ray sources will operate at very high repetition rate 100 MHz, with 200 pC electron bunches that means very high average current 20 mA.

These Compton sources are designed to operate with an electron energy range of 30-100 MeV, which for a 20 mA of current means 2 MW. Such a high beam power cannot be dumped without deceleration, and together with the CW (Continuous Wave) regime, it justifies to foresee an ERL (Energy Recovery Linac) machine, like in the CBETA ERL project [4].

The focus on enabled applications by such an energy range and brilliance is on medical oriented research/investigations, mainly in the radio-diagnostics and radio-therapy fields [5,6], exploiting the unique features of monochromatic X-rays, as well as in micro-biological studies, and, within this mainstream, material studies, crystallography and museology for cultural heritage investigations. In this paper, the layout and

the typical parameters of the BriXS X-ray source will be discussed.

### MACHINE LAYOUT

The BriXS layout, shown in Figure 1, consists of two symmetric beam lines, fed by two independent photoinjectors, where two equal and coupled Energy Recovery Linacs (ERL) accelerate the electron beams. Electron trains are extracted from the photo-cathodes Inj1 and Inj2 at the left side of in Figure 1. The two ERLs (named ERL1 and ERL2 in the Figure) accelerate and decelerate the electron trains in an unconventional push-and-pull scheme. Bunches from Guns and travelling right away in the Figure are accelerated, those coming back from the interaction points (IPs) are decelerated during the energy recovery phase and brought simultaneously to a single beam-dump. Each Linac is therefore traversed by two counter-propagating trains of electron beams, both gaining and yielding energy. This push-and-pull coupled scheme permits to concurrently drive two Compton X-ray sources with the same degrees of freedom, in terms of energy and electron beam quality, as a Linac driven source, with the advantage that the coupled ERLs scheme, fed by two independent RF, systems is more stable. CW electron Guns, capable to produce such an average beam current, are not yet state of the art. Some of the most promising photo cathode Guns [7] as the Cornell DC Gun [8] and the RF-CW Apex Gun [9] have been therefore compared by simulations. Considering the simulations results was chosen the APEX one. Partial modifications of the beam lines to host additional Compton interaction points are under study. BriXS should be considered as a single folded ERL running two beams. This scheme is more compact than two independent ERLs, with the necessity of less magnetic elements and, therefore, a minor cost. An important advantage is that the present scheme provides two knobs for adjusting the phases at the entrance of the linacs in the recovery stage, thus circumventing the necessity of additional matching lines for running one single ERL at different energies.

### INJECTOR

Two twin injectors are present in BriXS. The injector layout of the BriXS/MariX common acceleration beam-line, as sketched in Figure 2, is composed of the following accelerating and focusing elements: 1. The CW RF Gun; 2.

\* illya.drebot@mi.infn.it

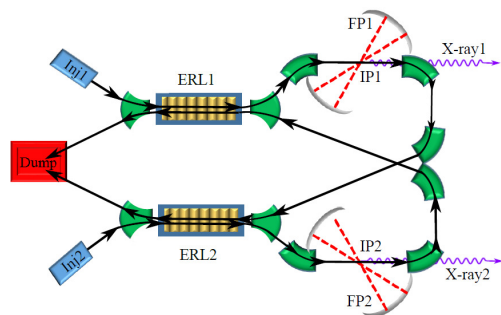


Figure 1: Pictorial view of the BriXs layout: From the left side: Inj1 and Inj2: photocathodes. ERL1 and ERL2: Superconducting Linacs. FP1 and FP2: Fabry-Pérot cavities. IP1 and IP2: interaction points. X-ray1 and X-ray2: X rays beams, going towards Compton users areas.

Two focusing solenoids; 3. One RF buncher; 4. Two linear accelerators; 5. One RF linearizing cavity. Being two identical beamlines, we show and discuss only one from here on for simplicity. The RF power source for each component of the BriXS injector operates in CW, since the high repetition rate (100 MHz) electron beam reaches an average power of 120 kW at the exit, i.e. energy up to 6 MeV and average current of 20 mA. Therefore, the choice of the RF system is based on the maximum average RF power that can be handled by the RF devices. The CW RF-Gun and the RF Buncher are based on normal conducting (NC) technology, since the RF power dissipated inside the cavities, required to accelerate and to bunch the electron beam with an energy of about 800 keV at the beginning, can be still handled by using standard water-cooling systems. The APEX Gun [9] has already shown operation at about 87 kW of average dissipated RF power with the possibility to operate even up to 100 kW. As for the two linacs and the RF linearizer, where the high rep-rate beam is accelerated up to at least 6 MeV, we have decided to use superconducting (SC) technology since standard copper structures are not able to dissipate the high average RF power that would be required. Indeed, the cavity wall power consumption inside a SC structure is lower than a NC one by a factor of  $10^5 - 10^6$ .

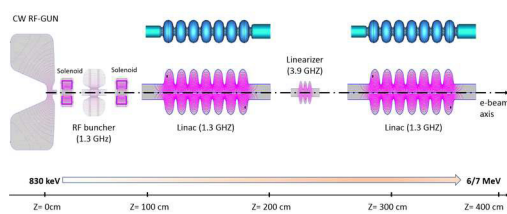


Figure 2: Injector layout for 1 beam-line, SuperFish 2D model.

## ACCELERATOR SECTION

The requirement for a CW beam structure imposes the choice of the Superconducting technology for the accelerat-

ing section, in order to save in capital and operational cost because we want to operate at an accelerating gradient of at least 15 MV/m. This technology has been developed over the past thirty years and has now reached a mature status. The latest most important high repetition rate or CW accelerator facilities (E-XFEL, LCLS-II, ESS, etc.) are now based on this consolidated technology.

To provide the required 100 MeV maximum energy, we need to consider two important aspects for the selection of the accelerating structure, namely the requirement for RF operation and the effect of the induced High Order Modes on the beam quality. The choice of the BriXS accelerating structure is determined by the above considerations and by the performance already achieved in structures used in installations similar to BriXS. We have evaluated, for this case, two experimentally tested different cavity/module designs:

- Compact ERL(KEK), 100 mA current target still to be demonstrated. The based accelerating unit is a cryomodule with two 9-cells cavity design to suppress HOM-BBU up to the nominal current (theoretical limit is 200 mA). It has demonstrated an up to 1 mA CW operation with a  $100.0 \pm 0.03\%$  energy recovery and providing a 15 MV/m accelerating gradient. The TESLA-geometry cavity has been modified to accommodate two HOM absorber able to dissipate up to 150 W. These cavities are operated at 2.0 K.
- CBETA (Cornell), multi-pass ERL demonstrator, linac module tested, Design Report. Each module consists of six 7-cell cavities, designed to operate in CW mode at 16 MV/m with a HOM-BBU limit at 100 mA. Specifically designed HOM absorbers installed on both side are able to handle up to 400 W of dissipated power. These absorbers are isolated from the cavity and they are eventually cooled with liquid nitrogen. The module has been successfully tested and has reached the designed performances. The cryogenic operation temperature for this project is 1.8 K.

In order to contain the overall module footprint, a solution adopting a single cryomodule hosting the required number of cavities is preferable. This would suggest to explore the opportunities offered by the six-cavities CBETA cryomodule given its demonstrated performance. However, with a 0.81 m single cavity active length, the CBETA cryomodule would yield a 77.8 MeV energy gain when operated at 16 MV/m accelerating gradient. An eight 7-cells cavities geometry CBETA cryomodule appears to be needed to fulfill the energy gain requirements for BriXS. It is clear that, while the CBETA cryomodule remains a reference design, dedicated developments are needed for the current project.

Dealing with the cryogenics losses we need to include the dynamic losses as well as the HOM power. The cryogenic dynamic losses per single cavity, based on the previous parameter set, are expected to be 9.3 W. For the HOM power, in the non-resonant monopole case, the CBETA cavity has a longitudinal loss factor of 14.7 V/pC [4]. Based on this

Table 1: BriXS Cavity Operational Parameters

Parameter	Value
Accelerating structure	Standing Wave
Accelerating mode	$TM_{0,1,0} \pi$
Fundamental frequency [GHz]	1.3
Energy gain per cavity [MeV]	12.5
Accelerating gradient $E_{acc}$ [MV/m]	15.6
Intrinsic quality factor $Q_0$	$2 \times 10^{10}$
Loaded quality factor $Q_{load}$	$3.25 \times 10^7$
Cavity half bandwidth at $Q_{load}$ [Hz]	20
Operating temperature [K]	1.8 (2.0)
Number of cells	7
Active length [m]	0.810
$R/Q$ (fundamental mode) [Ohm]	774
RF power per cavity [kW]	2.85
Dynamic cryogenic losses per cavity [W]	9.3
HOM cryogenic losses per cavity [W]	117
Cavity total longitudinal loss factor for $\sigma = 0.6$ mm [V/pC]	14.7
$Q$ [pC]	200.0
$f_{bunch}$ [MHz]	100
Average current [mA]	20

parameter, the estimated loss power is 117 W per cavity. This value can be reasonably handled by a CBETA-like solution for the HOM absorber made of SiC material and with a cooling jacket held at 80 K.

It is then clear that, if we opt to start from a proofed and operating cavity and cryomodule design, the CBETA layout guarantees these points and allows a smaller total length with respect to a solution like ERL(KEK). It is worth noting that modifications of the original CBETA design are necessary to reach the requested 100 MeV energy gain by implementing an 8 cavities per module structure. On the cavity side, we should keep in mind that the  $2 \times 10^{10}$  unloaded quality factor is achieved by operating the cavity at 1.8 K, while we are now aiming at operating BriXS at 2.0 K. While the CBETA cavity has shown to reach our specification also at 2.0 K, we are now considering to introduce an Electro Polishing process in the cavity treatment procedure (well established in the XFEL production). This will help achieving BriXS higher  $Q_0$  values and will give us more confidence in reaching the design unloaded  $Q$  value. In Table 1, we summarize the BriXS requirements and the accelerating section design parameters.

## ELECTRON BEAM LINES

The top view projection of the BriXS scheme, in the present configuration with two interaction points (IP) is shown in Figure 1. Each branch of the two BriXS beam lines, depicted in Figure 3, includes the following sections:

1. a quadrupole triplet, located downstream the SC Linac ERL1, matches the beam to the first chicane and al-

lows for quadrupole-scan emittance diagnostic; electron bunches travel through these elements in both directions, outgoing from the accelerator or backwards from the specular path;

2. a dog-leg chicane, composed of two 20° dipoles and three quadrupole lenses closing the chicane dispersion, transports the beam to the IP line;
3. the IP region includes two strong focusing triplets, symmetrically installed w.r.t. the IP, and the about 1 m long Fabri-Pérot Optical Cavity. This section has identity transport matrix, so different focusing settings at IP can be adopted without affecting the magnetic elements downstream.
4. a double bend achromat (DBA) section with two 90° dipoles and three quadrupoles deflects the beam by 180° and closes the dispersion at its end;
5. a long dog-leg chicane with two 20° dipoles translates the beam to the second SC Linac; the triplets provide control the clearance of the first quads to avoid interference at the X-cross of the two beam lines;
6. the triplets "1" in Figure 3 are identical and specular structures.

Each of the electron beam lines has been designed so that the dispersion is closed at the IP region, at the exit of the DBA (4), where a diagnostic station will be installed, and at the exit of the second chicane (5) in order to optimize the beam injection in the ERL.

The IP region is designed with possibility to install second IP what open a possibility to operate BriXS as two-colour X-ray source [10, 11].

The transport of the electron beam from the exit of the first ERL, through the IP to the entrance of the second ERL has been performed by Elegant [12] and is part of start to end simulations.

The main electron beam parameters at the IP are collected in Table 2.

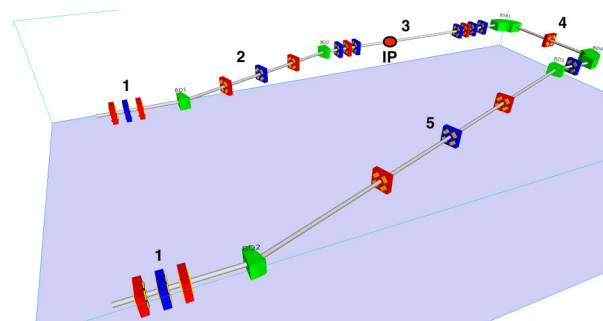


Figure 3: Scheme of the magnetic elements of a single BriXS beam line.

Table 2: Electron Beam Parameters at the Compton IP

Parameter	Value
Electrons mean energy [MeV]	30-100
Bunch charge [pC]	100-200
Emittance $\epsilon_{nx}, \epsilon_{ny}$ [mm mrad]	0.6-1.5
Relative energy spread $\sigma_e$ [%]	$10^{-2} - 10^{-1}$
Focal spot size $\sigma_x, \sigma_y$ [ $\mu\text{m}$ ]	19.4-23.4
Bunch length rms [ $\mu\text{m}$ ]	400-900
Repetition rate [MHz]	100

## EXPECTED PERFORMANCE

The working point is the result of a full start-to-end simulation along all the BriXs electron beam line, from the photocathode to the radiation detector. The electron bunch parameters at IP used in this simulation, as well as the laser and the radiation characteristics, are presented in the first seven lines of Table 3. The Compton emission has been simulated using the Monte Carlo code CAIN [13].

Due to the boosted nature of the Compton back scattering process,

$$E_{ph} = \frac{2E_L \gamma^2 (1 + \cos \alpha_0)}{1 + \gamma^2 \theta^2}, \quad (1)$$

where  $\gamma$  is electron Lorentz factor,  $\alpha_0$  is interaction angle,  $\theta$  is emission angle, the radiation exhibits an energy-angle correlation with the most energetic photons emitted on axis, while the outer regions are occupied by low energy photons. This feature makes possible to get monochromatic radiation by inserting irides or collimators along the path of the radiation, selecting therefore only the photons within a given collimation angle  $\theta_{max}$ .

Figure 4 presents the spectrum of the radiation collimated respectively in the angles:  $\theta_{max} = 0.6$  mrad, leading to a bandwidth of 1%,  $\theta_{max} = 2.9$  mrad with  $bw = 5\%$  and  $\theta_{max} = 3.9$  mrad with a corresponding bandwidth of 10%. The number of collimated photons per shot, about  $5 \times 10^3$  in 1% bandwidth, increases to  $4.7 \times 10^4$  for 5% of bandwidth and to  $8.4 \times 10^4$  for 10% of bandwidth, giving respectively  $5 \times 10^{11}$ ,  $4.7 \times 10^{12}$  and  $8.4 \times 10^{12}$  photons per second.

The dependence of the number of the scattered photons  $N_{ph}$ , bandwidth  $bw$  and average Stoke parameter  $\langle S_x \rangle$  on the collimation angle  $\theta_{max}$  is reported in Figure 5. The polarization [14] slightly decreases with increasing angles, but remains always in total well above 80% and even more in the collimated region. The photon intensity on a screen perpendicular to the electron beam at various distances are presented in Figure 6.

## BRIXSINO

BriXsinO, as a reduced scale demonstrator of the modified push-pull folded ERL scheme with maximum energy of electrons 8-10 MeV. The layout of it presented in Figure 7. The specific goal of this demonstrator compact machine is to investigate RF mode stability issues in the CW energy

Table 3: Parameters of Start to End Simulations for the High Energy WP

Electron beam Parameters			
Electrons mean energy (MeV)	100		
Bunch charge (pC)	200		
Normalized emittance $\epsilon_{nx}, \epsilon_{ny}$ (mm mrad)	1.2, 1.2		
Relative energy spread $\sigma_E/E$	$1.6 \times 10^{-2}$		
Bunch length rms ( $\mu\text{m}$ )	440		
Focal spot size $\sigma_x, \sigma_y$ ( $\mu\text{m}$ )	19.4, 23.4		
Repetition rate (MHz)	100		
Laser Parameters			
Laser pulse energy (mJ)	7.5		
Laser wavelength (nm)	1030		
Laser pulse length (ps)	2		
Laser focal spot size $w_{0x}$ ( $\mu\text{m}$ )	40		
Laser focal spot size $w_{0y}$ ( $\mu\text{m}$ )	80		
Collision angle (deg)	7		
$\gamma$ -ray Photon beam Parameters			
Relative bandwidth rms %	1	5	10
Absolute bandwidth rms (keV)	1.98	8.66	16.01
Absolute bandwidth FWHM (keV)	3.51	22.7	47.67
Collimation angle $\theta_{max}$ (mrad)	0.6	2.08	3.3
Peak photon energy (keV)	183.4	182.4	180.4
Mean photon energy (keV)	181.0	170.4	158.7
Photon number per shot $N_{Tot}$	$2.5 \times 10^5$		
Photon number per shot after collimation $N_{ph}$	$5 \times 10^3$	$4.7 \times 10^4$	$8.4 \times 10^4$
Source rms size $\sigma_{\gamma x}, \sigma_{\gamma y}$ at IP ( $\mu\text{m}$ )	19.6, 16.7		
Source rms divergence $\sigma_{\gamma x'}, \sigma_{\gamma y'}$ ( $\mu\text{rad}$ )	0.3, 0.3	1.0, 1.0	1.6, 1.3
Source rms divergence $\theta_{rms}$ ( $\mu\text{rad}$ )	0.42	1.41	2.08
Spot Size at 10 m (mm)	3.0, 3.0	10.5, 9.44	16.3, 13.0
Rad. pulse length $\sigma_{\gamma z}$ (ps)	1.35		

recovery operating mode at high average current and very high repetition rate for the electron beam (up to 100 MHz), and related impacts on the electron beam quality (emittance, energy spread) due to beam break-up effects and beam loading. The main issues to be addressed by the test-bench demonstrator BriXsinO include: a) Achievement of electron beam quality (emittance, energy spread), as requested by an optimal luminosity in the ICS. b) Stability of RF, phasing

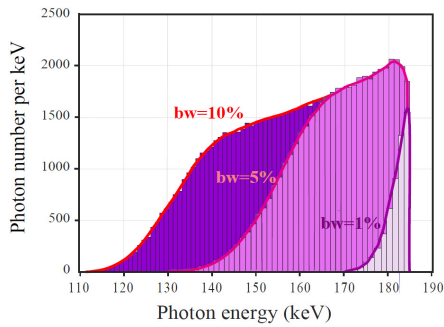


Figure 4: Spectrum of collimated scattered photons for the high energy case  $E_e = 100$  MeV. Violet histogram:  $bw = 10\%$ ,  $\theta_{max} = 3.3$  mrad; magenta histogram:  $bw = 5\%$ ,  $\theta_{max} = 2.08$  mrad; grey histogram:  $bw = 1\%$ ,  $\theta_{max} = 0.6$  mrad.

and timing of beam energy recovery in the folded push-pull ERL scheme. c) Photo-cathodes and RF-Gun capabilities to generate 100 MHz electron beams. d) Beam quality preservation with and without ERL (beam-breakup, beam loading). e) Options of two-color ICS generation. f) Radio-protection evaluation with deaccelerated beam after energy recovery.

## CONCLUSIONS

In this paper the conceptual design of the compact X-ray Source BriXS (Bright and compact X-ray Source) is presented. BriXS, the first stage of Marix project, is a Compton X-ray source based on superconducting cavities technology for the electron beam with energy recirculation and on a laser system in Fabry-Pérot cavity at a repetition rate of 100 MHz, producing 20-180 keV radiation for medical applications. An energy recovery scheme based on a modified folded push-pull CW-SC twin Linac ensemble allows to sustain MW-class beam power with almost just one hundred kW active power dissipation/consumption.  $5 \times 10^4 - 10^5$  collimated photons per shot in a bandwidth of 5 - 10% are produced with  $10^8$  repetition rate for a total amount of more

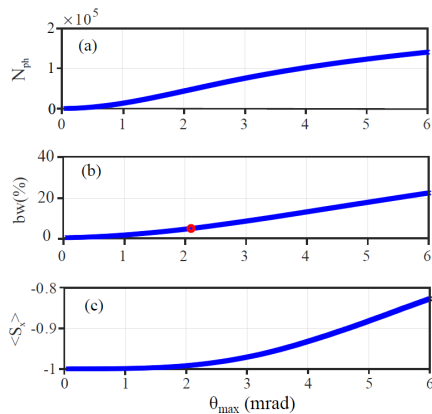


Figure 5: High energy case  $E_e = 100$  MeV. (a) Number scattered photons, (b) bandwidth and (c) average Stoke parameter as function of collimator angular aperture  $\theta_{max}$ .

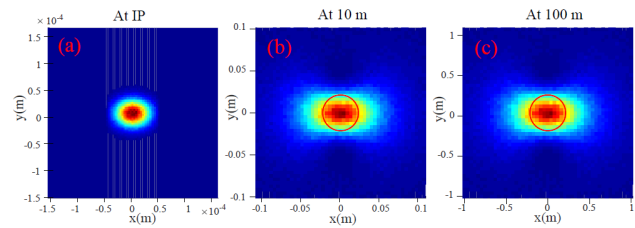


Figure 6: Photon intensity on a screen perpendicular to the electron beam. (a): at the interaction point (IP); (b): at 10 m from the source; (c) at 100 m. The red circle delimits the region inside the  $\theta=1/\gamma$  acceptance angle.

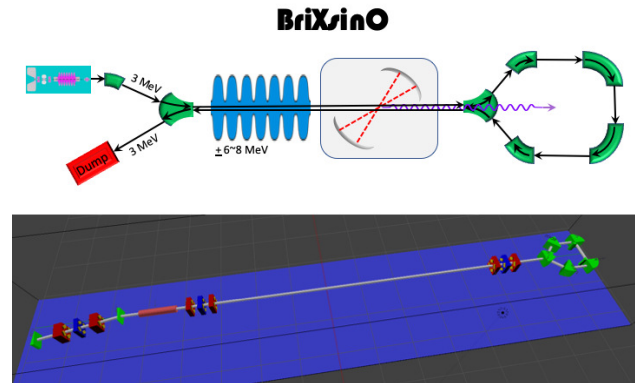


Figure 7: Layout of BriXsinO.

than  $10^{13}$  photons per second, a performance comparable to the most advanced X-rays sources. An adjoint possibility is the production of two color radiation for imagine application.

## REFERENCES

- [1] MARIX Conceptual Design Report, 2019, [www.marix.eu](http://www.marix.eu)
- [2] L. Serafini, *et al.*, “MariX, an advanced MHz-class repetition rate X-ray source for linear regime time-resolved spectroscopy and photon scattering”, NIM, A930, 2019, p 167-172. doi: 10.1016/j.nima.2019.03.096
- [3] L. Serafini *et al.*, “The MariX source (Multidisciplinary Advanced Research Infrastructure with X-rays)”, in *Proceedings of IPAC2018*, Vancouver, Canada, 2018. doi:10.18429/JACoW-IPAC2018-THPMF058
- [4] G. Hoffstaetter, *et al.*, “CBETA Design Report”, USDOE - OSTI, BNL-114549-2017-IR, June 2017. doi:10.2172/1412725
- [5] G. Mettievier, *et al.*, “[OA192] Kilovoltage rotational radiotherapy with the marix/brixs source for partial breast irradiation”, *Physica Medica*, Volume 52, Supplement 1, 2018, Page 74. doi:10.1016/j.ejmp.2018.06.264
- [6] G Paternó, *et al.*, “Inverse Compton radiation: a novel x-ray source for K-edge subtraction angiography?”, *Physics in Medicine & Biology*, V. 64, 2019. doi:10.1088/1361-6560/ab325c
- [7] B. Dunham *et al.*, “Record high-average current from a high-brightness photoinjector”, in *Applied Physics Letters* 102.3 (2013), p. 034105. doi:10.1063/1.4789395

Content from this work may be used under the terms of the CC BY 3.0 licence (© 2019). Any distribution of this work must maintain attribution to the author(s), title of the work, publisher, and DOI

- [8] C. Gulliford *et al.*, “Demonstration of cathode emittance dominated high bunch charge beams in a DC gun-based photoinjector”, in *Applied Physics Letters*, 106.9 (2015), p. 094101. doi:10.1063/1.4913678
- [9] F. Sannibale *et al.*, “Upgrade Options Towards Higher Fields and Beam Energies for Continuous-Wave Room-Temperature VHF RF Guns”, in *8th Int. Particle Accelerator Conf.(IPAC’17)*, Copenhagen, Denmark, 2017. doi:10.18429/JACoW-IPAC2017-MOPIK019
- [10] I. Drebot, V. Petrillo, and L. Serafini, “Two-colour X-gamma ray inverse Compton back-scattering source”, in *EPL (Europhysics Letters)*, 120.1 (2017), p. 14002. doi:10.1209/0295-5075/120/14002
- [11] I. Drebot *et al.*, “Multi Colour X-Gamma Ray Inverse Compton Back-Scattering Source”, in *Proceedings of IPAC2018*, Vancouver, Canada. doi:10.18429/JACoW-IPAC2018-THPMF057
- [12] M. Borland, “Elegant: A flexible SDDS-compliant code for accelerator simulation”, USDOE - OSTI, LS-287, 2000. doi:10.2172/761286
- [13] P. Chen *et al.* “CAIN: Conglomerat d’ABEL et d’Interactions Non-lineaires”. In: *Nuclear Instruments and Methods in Physics Research Section A: Accelerators, Spectrometers, Detectors and Associated Equipment* 355.1 (1995), pp. 107–110. doi:10.1016/0168-9002(94)01186-9
- [14] V. Petrillo *et al.* “Polarization of x-gamma radiation produced by a Thomson and Compton inverse scattering”. In: *Physical Review Special Topics-Accelerators and Beams* 18.11 (2015), p. 110701. doi:10.1103/PhysRevSTAB.18.110701